

## SU(2) uncertainty limits

Saroosh Shabbir\* and Gunnar Björk

*Department of Applied Physics, Royal Institute of Technology (KTH)  
AlbaNova University Center, SE - 106 91 Stockholm, Sweden*

(Dated: June 11, 2022)

Although progress has been made recently in defining non-trivial uncertainty limits for the SU(2) group, not much work has been done to describe the behaviour of the intermediate states bound by these limits. In this paper we systematically calculate the variance of the SU(2) operators for all states belonging to the  $N = 2$  and  $N = 3$  polarisation excitation manifold (corresponding to spin 1/2 and spin 1) and present the permissible values for all pure states. We demonstrate that all states on the same orbit, i.e. all states reachable via an SU(2) transformation, have the same sum variance which provides useful experimental information for realisable quantum experiments. Lastly, and perhaps counter to expectation, we note that even pure states can reach the maximum uncertainty limit.

PACS numbers: 42.50.Tx, 03.65.-w, 42.50.Xa

The algebra of SU(2) is ubiquitous in Physics, describing, among other phenomenon, the angular momentum characteristics of atomic systems. Formally equivalent to the angular momentum operators are the Stokes parameters that describe the polarisation state of light. In classical optics, the degree of polarisation has been defined as the length of the Stokes vector. This quantitative measure of polarisation has been found to be insufficient in the quantum domain; states which appear unpolarised have been shown to possess polarisation structure via higher (than dipolar) order correlation measurements [1–3]. Thus, it is essential to consider quantum fluctuations of the Stokes operators to arrive at an operationally adequate description of polarisation in the quantum domain. Moreover, quantum fluctuations of angular momentum operators, and hence their associated uncertainty relations, also play a crucial role in metrology, where they define the ultimate limit to the resolution of interferometric measurements [4–6]. In this letter, we study the second order statistics to arrive at non-trivial limits for the uncertainty relation for the Stokes observables and detail the states that reside within these limits.

In some sense the uncertainty relations in quantum mechanics embody the departure from the classical world. They describe the impossibility of simultaneous sharp preparations of incompatible observables as embodied in the Robertson-Schrödinger (R-S) uncertainty relations [7, 8]. However, in contrast to the canonical uncertainty relations involving position and momentum observables,  $\Delta x \Delta p_x \geq \hbar/2$ , the uncertainty relations for the SU(2) group give state-dependent bounds which can lead to trivial results. Moreover these uncertainty relations are not unique. Below we present a framework to address these issues.

Non-canonical uncertainty relations have been studied in various ways. One approach has been to look at the states saturating the R-S uncertainty relation [9–11] named as “intelligent states” [9]. However, the class of intelligent states seems to lack any natural application. Another approach has been to form weighted uncertainty relations [12]. These sometimes provide sharper bounds than the Robertson-Schrödinger relations, but at the expense of weighing the operators unequally. An experimental justification for doing so is presently lacking. In [13] uncertainty limits were derived for an arbitrary number of non-commuting observables, but the limits were state dependent, just as in the intelligent state approach. Pati *et al.* [14] have used another approach and derived the uncertainty limits for a joint measurement of many identical copies of a certain state. They have shown that such a joint measurement of  $N$  identical systems will have an uncertainty a factor of  $N^{-1/2}$  smaller than if each of the  $N$  systems were measured individually and these  $N$  measurement values were used to estimate the value of the measured observable.

Our approach in this work is to some extent similar to Wünsche’s who has derived higher order uncertainty relations for a variety of algebras from invariants [15]. Specifically, much of the algebra needed to derive our relations is found in [6], where the authors looked at the ultimate measurement precision of angular momentum operators, which apart from a factor of 1/2 are identical to the Stokes operators. The alternative method of quantifying uncertainties via entropic uncertainty relations has also been studied extensively [16–18], however here we restrict ourselves to non-entropic measures.

For the monochromatic field of light in two orthogonal modes, the Stokes operators [19, 20] can be succinctly represented as

$$\hat{S}_\mu = (\hat{a}_R^\dagger \ \hat{a}_L^\dagger) \sigma_\mu \begin{pmatrix} \hat{a}_R \\ \hat{a}_L \end{pmatrix}, \quad (1)$$

where  $\hat{a}_R$  and  $\hat{a}_L$  are the annihilation operators of right

---

\* e-mail:saroosh@kth.se

(R) and left handed (L) circular polarisation modes. The Greek letter  $\mu$  runs from 0 to 3 with  $\sigma_0 = 1$ , and  $\sigma_k$ ,  $k \in \{1, 2, 3\}$ , are the Pauli matrices.  $\hat{S}_0$  then defines the total number of photons and the Stokes vector  $\langle \hat{\mathbf{S}} \rangle = \langle \hat{S}_1, \hat{S}_2, \hat{S}_3 \rangle$  indicates the polarisation in horizontal/vertical, diagonal/anti-diagonal and left-circular/right-circular modes respectively. (The Gell-Mann boson representation of the angular momentum operators are smaller than the Stokes operators by a factor of 1/2 but otherwise identical.)  $\hat{S}_k$  satisfy the commutation relations of the SU(2) algebra:  $[\hat{S}_k, \hat{S}_l] = i\epsilon_{klm}\hat{S}_m$ , where  $\epsilon_{klm}$  is the Levi-Civita fully antisymmetric tensor. Since the commutation relation is state-dependent, so is the uncertainty limit for the Stokes (or angular momentum) operators. Viz.,

$$\Delta S_k \Delta S_l \geq \frac{1}{2} \left| \epsilon_{klm} \langle \hat{S}_m \rangle \right|^{1/2}, \quad (2)$$

where  $\Delta S_k = (\langle \hat{S}_k^2 \rangle - \langle \hat{S}_k \rangle^2)^{1/2}$ . Thus, the uncertainty limit depend on the state, as mentioned above.

Complete second order statistics of the polarisation observables can be extracted from the  $3 \times 3$  covariance matrix [6, 21, 22],

$$\Gamma_{kl} = \langle \hat{S}_k \hat{S}_l + \hat{S}_l \hat{S}_k \rangle / 2 - \langle \hat{S}_k \rangle \langle \hat{S}_l \rangle. \quad (3)$$

It's utility stems from its simple connection to measurements and, moreover it's Hermitian by construction. Since it is a second-rank tensor, we can readily define three invariants; the determinant, the sum of the principle minors and the trace. Expressed in terms of the eigenvalues  $\lambda_k$  of  $\Gamma$ ,  $k \in \{1, 2, 3\}$ , these can be used to form state-dependent uncertainty relations, viz:

$$0 \leq \lambda_1 \lambda_2 \lambda_3 \leq \langle \hat{S}_0^3 (\hat{S}_0 + 2)^3 \rangle / 27, \quad (4)$$

$$\hat{S}_0^2 \leq \lambda_1 \lambda_2 + \lambda_2 \lambda_3 + \lambda_3 \lambda_1 \leq \langle \hat{S}_0^2 (\hat{S}_0 + 2)^2 \rangle / 3, \quad (5)$$

$$\langle \hat{S}_0 \rangle \leq \lambda_1 + \lambda_2 + \lambda_3 \leq \langle \hat{S}_0 (\hat{S}_0 + 2) \rangle, \quad (6)$$

where  $\lambda_1, \lambda_2$  and  $\lambda_3$  are the (real and non-negative) eigenvalues of the covariance matrix. However, while the relations are state dependent all three relations are invariant under any polarisation transformation. We will come back to this important point below.

Out of these three equations only the last one, Eq. (6), gives non-trivial bounds, encompassing the extrema of the other two. For example, the lower limit of (4) follows from the non-negativity of the eigenvalues, and this limit is reached for all SU(2) coherent states that are eigenstates of one of the Stokes operators and thus have zero variance in that observable. Given the constraint

$\lambda_1 + \lambda_2 + \lambda_3 \leq \langle \hat{S}_0 (\hat{S}_0 + 2) \rangle$  from (6) and the fact that the eigenvalues are real and non-negative, choosing the eigenvalues to be equal, i.e.,  $\langle \hat{S}_0 (\hat{S}_0 + 2) \rangle / 3$ , will maximize their product. The upper limit of (4) follows, and this limit is reached by pure states such as the polarisation NOON-states  $(|N, 0\rangle + |0, N\rangle) / \sqrt{2}$  which is perhaps counter-intuitive since one would expect the uncertainty to be maximum for only mixed states. In the following we use (6) to demonstrate the uncertainty structure of all pure states for a given excitation manifold.

The Poincaré sphere affords an elegant pictorial representation of the polarisation state of light. Each of the Stokes operators define the polarisation of the state along the three coordinate axes of the Poincaré Sphere. The polarisation characteristics of a single photon are represented by a point on or within the surface of the Poincaré sphere. For  $N > 1$ , any pure, two-mode state can be represented on the Poincaré sphere via its Majorana representation [23, 24] which maps the  $N$ -photon state as  $N$  points on the surface of the sphere. We know that any general, pure, two-mode  $N$ -photon state can be expressed as [25, 26]

$$\begin{aligned} |\psi\rangle &= \sum_{n=0}^N c_N |n, N-n\rangle \\ &= \frac{1}{\sqrt{\mathcal{N}}} \prod_{n=1}^N \left( \cos(\theta_n/2) \hat{a}_R^\dagger + \exp(i\phi_n) \sin(\theta_n/2) \hat{a}_L^\dagger \right) |0, 0\rangle, \end{aligned} \quad (7)$$

where  $\mathcal{N}$  is the normalisation factor. Each of the factors in the above equation can be represented as a point on the Poincaré sphere with coordinates  $(\sin(\theta) \cos(\phi), \sin(\theta) \sin(\phi), \cos(\phi))$ . For example, the Majorana representation of  $N$ -photon SU(2) coherent state,  $|\Psi_{\text{SU}(2)}\rangle = (N!)^{1/2} (\hat{a}_R^\dagger)^N |0, 0\rangle$ , is a collection of  $N$  points stacked on top of each other at the North pole of the Poincaré sphere, in line with the intuitive description of SU(2) coherent states as exhibiting the most classical behaviour with their Stokes vector pointing in one particular direction.

At the opposite end, SU(2) maximally unpolarized, pure states have vanishing Stokes vector and isotropic variance (for  $N > 3$ ), i.e. their polarisation up to second order points nowhere [24, 27]. The Majorana representation of these states is comprised of points spread as symmetrically as possible over the surface of the Poincaré sphere. For certain excitations greater than 3, these points form the vertices of the Platonic solids. Somewhere in-between these two extremes is the  $N$ -photon NOON state,  $|\Psi_{\text{NOON}}\rangle = (2N!)^{1/2} ((\hat{a}_R^\dagger)^N + (\hat{a}_L^\dagger)^N) |0, 0\rangle$  which is represented by  $N$  equidistant points along the equator. It is because of this configuration that NOON states have the highest sensitivity to small rotations about  $\hat{S}_3$  [27], thus underscoring their metrological importance. Similar to the biphotons  $|1, 1\rangle$  generated in spontaneous parametric down conversion, the NOON states manifest hidden polarisation [1] for  $N \geq 2$ . All of these have vanishing Stokes vector but do

indeed show polarisation structure with higher order polarisation correlation measurements such as the variance.

In terms of the Stokes operators any general, linear polarisation transformation can, e.g., be written as:

$$\hat{U}_{Pol} = \exp(i\alpha\hat{S}_3) \exp(i\beta\hat{S}_2) \exp(i\gamma\hat{S}_3) \quad (8)$$

Such transformations rotate the input state around  $\hat{S}_3$  by an angle  $2\gamma$ , followed by a rotation around  $\hat{S}_2$  by  $2\beta$  followed by a final rotation again around  $\hat{S}_3$  by  $2\alpha$ . From this two conclusions follow: First, an  $SU(2)$  transformation rigidly rotates the configuration of the points represented by (7), resulting in a different state on the same  $SU(2)$  orbit as the original state. To state explicitly, an orbit is the locus of  $SU(2)$  transformations for a particular state. Described another way, an orbit is a set of all states that are mutually convertible via  $SU(2)$  transformations. Second, different orbits are parametrised by different relative orientations of the Majorana points with respect to each other on the Poincaré sphere. For  $N = 2$ , there is only one relevant parameter governing the orientation of the two points with respect to each other - the angle  $\theta$  subtended by the two points at the centre of the sphere. The most general representation of the  $N = 2$  orbit generating state can thus be given by fixing one of its Majorana points at the North pole and constraining the other to move on the Greenwich-Meridian. This allows us to write the orbit generating state for the  $N = 2$  manifold as:

$$|\Psi_{N=2}\rangle = \frac{1}{\sqrt{N}} \hat{a}_R^\dagger \left( \cos(\theta/2) \hat{a}_R^\dagger + \sin(\theta/2) \hat{a}_V^\dagger \right) |0,0\rangle \quad (9)$$

Consequently, states with different  $\theta$  lie on different

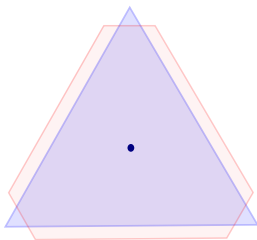


FIG. 1. Convex hull of the allowed variances. The eigenvalues of the covariance matrix form the vertices of the polygons. In case of threefold degeneracy, one obtains the point in the middle. The triangle is formed in the case of twofold degeneracy via cyclic permutation of the eigenvalues. If all three eigenvalues are distinct, one obtains the irregular hexagon. For  $N \geq 3$ , the figure also demonstrates the situation of overlapping orbits (for more information see text).

$SU(2)$  orbits. By definition states on the same  $SU(2)$  orbits have the same properties for invariants such as the eigenvalue sum (6). This sum, being the trace of a tensor, moreover is always equal to the sum of the variances for any state. Hence,  $(\Delta S_1)^2 + (\Delta S_2)^2 + (\Delta S_3)^2$  is a constant on every orbit.

We know that the  $N$ -photon  $SU(2)$  coherent states and the  $N$ -photon NOON states saturate the lower and upper limits of Eq. (6), respectively. To study the intermediate states, we calculate the covariance matrix as a function of the orbit generating parameter. The eigenvalues of the covariance matrix  $(\lambda_1, \lambda_2, \lambda_3)$  give the extrema of the Stokes operator variances. These can be permuted by applying the polarisation transformations that rotate the state around a particular Stokes-operator axis by  $\pm\pi/2$ . In variance space, using permutations of eigenvalues as the vertices, the so-constructed polygon is the convex hull of the allowed variances for a given orbit. Thus, all the points inside the polygon including the border are reachable from any other point on the polygon via an  $SU(2)$  transformation. If the eigenvalues are threefold degenerate,  $\lambda_1 = \lambda_2 = \lambda_3$ , one obtains a point (Fig. 1). In other words such an orbit has isotropic variance that will not change under any polarisation rotation. Doubly degenerate eigenvalues lead to a triangle in variance space. The triangle's surface normal will point in the direction  $(1, 1, 1)$  in the variance space formed by the axes  $(\Delta S_1)^2$ ,  $(\Delta S_2)^2$ , and  $(\Delta S_3)^2$ , thus keeping the variance sum constant on the triangle surface. In the case of no eigenvalue degeneracy, the orbit defines a triangle with chopped corners (in general, an irregular hexagon) in variance space, again oriented in the  $(1, 1, 1)$ -direction.

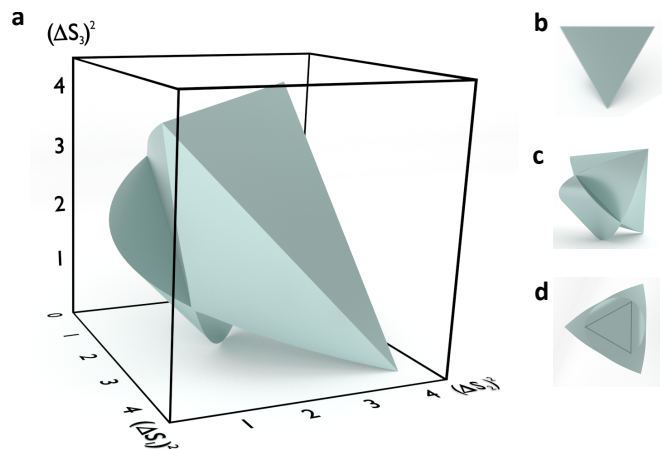


FIG. 2. (a) Permissible uncertainty values for the  $N = 2$  excitation manifold. (b) Top view with surface normal in the  $(1,1,1)$  direction, corresponds to the orbit for the NOON state. (c) Side view. (d) Bottom view with surface normal again in the  $(1, 1, 1)$  direction. The drawn triangle shows the orbit for the  $SU(2)$  coherent state.

Fig. 2 shows the shape of the volume in which all permissible triplets of variances  $((\Delta S_1)^2, (\Delta S_2)^2, (\Delta S_3)^2)$  must lie for  $N = 2$ . The cross-section normal to the variance space diagonal is the polygon circumscribing each orbit. The polygon closest to the origin is a triangle, with variance sum 4 and the vertices  $(2,2,0)$ ,  $(2,0,2)$  and  $(0,2,2)$ . As expected, it represents the  $SU(2)$  coherent state  $|2,0\rangle$  and its  $SU(2)$  orbit. The polygon furthest from the origin is also a triangle, with variance

sum 8 and the vertices at  $(4,4,0)$ ,  $(4,0,4)$  and  $(0,4,4)$ . This triangle represents the state  $|1,1\rangle$  and its orbit. On each orbit one can quite obviously find a state which has  $(\Delta S_1)^2 = (\Delta S_2)^2 = (\Delta S_3)^2$ . However, for  $N = 2$  the parameter space is too small to allow for complete isotropy, that is, an orbit with invariant Stokes variances.

The Majorana representation of 3 points corresponds to a triangle on the surface of the Poincaré sphere, and

$$|\Psi_{N=3}\rangle = \frac{1}{\sqrt{N}} \hat{a}_R^\dagger \left( \cos(\theta_2/2) \hat{a}_R^\dagger + \sin(\theta_2/2) \hat{a}_L^\dagger \right) \left( \cos(\theta_3/2) \hat{a}_R^\dagger + \exp(i\phi_3) \sin(\theta_3/2) \hat{a}_L^\dagger \right) |0,0\rangle, \quad (10)$$

where one can use the restriction  $\theta_2 \leq \theta_1$  to eliminate some of the degeneracy this parameterisation leads to. It is also possible to restrict  $\phi \leq \pi$  since point configurations obeying mirror symmetry define identical uncertainty limits although they don't belong to the same orbit.

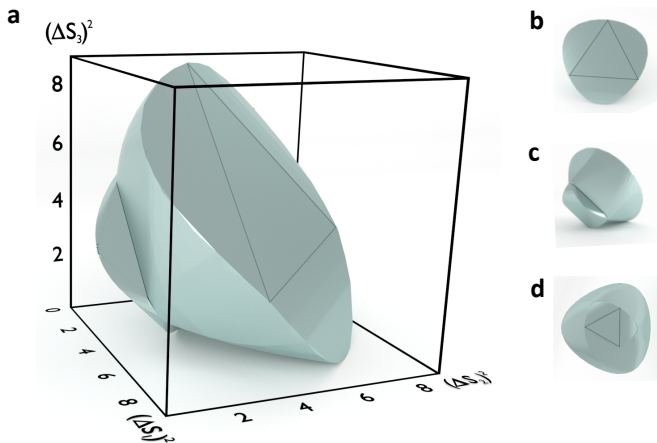


FIG. 3. (a) Permissible uncertainty volume for the  $N = 3$  manifold. (b) Top view with surface normal in the  $(1,1,1)$  direction. The drawn triangle shows the orbit for the NOON state. (c) Side view. (d) Bottom view with surface normal again in the  $(1,1,1)$  direction. The orbit for the  $SU(2)$  coherent state is shown.

We see that the permissible uncertainty values for  $N = 3$  has a similar structure as for the  $N = 2$  case (Fig. 2). However, one of the primary distinctions is that in contrast to the  $N = 2$  case, the cross-section normal to the space diagonal is composed of two or more overlapping orbits. As a consequence, different orbits may have the same variance sum as illustrated in Fig. 1 where, e.g. one orbit could have its permissible variances bounded by a triangle, while a different orbit with the same sum variance may be bounded by an irregular hexagon. Thus, equal sum variance is not a sufficient condition for two states to be on the same orbit and thus be mutually transformable via an  $SU(2)$  transformation.

A interesting state in the  $N = 3$  excitation manifold is

as a result the orbit generating state for  $N = 3$  is a function of three parameters. Following the same idea as for the  $N = 2$  case, we fix one point on the North pole ( $\theta_1 = \phi_1 = 0$ ). The second is constrained to move on the Greenwich-Meridian ( $\phi_2 = 0$ ) and the third is nominally allowed all possible  $\theta$  and  $\phi$  configurations. Accordingly, the orbit generating state for the  $N = 3$  manifold is given as follows:

the state

$$(0, -0.273055 + 0.573292i, 0.265388 + 0.420356i, 0.591310), \quad (11)$$

expressed in the basis  $\{|0,3\rangle, |1,2\rangle, |2,1\rangle, |3,0\rangle\}$ , where the left (right) index in the ket indicates the number of right-hand (left-hand) polarized photons. This state belongs to an orbit with a polarisation transformation-invariant Stokes operator variance. The state has a non-vanishing Stokes vector  $((1.22, -1.93, 0.89))$ , and is thus not even first order unpolarized, but yet, any polarisation transformation will yield the variance  $\Delta S_k^2 = 3$ ,  $k \in \{1, 2, 3\}$  invariant. The state may be interesting for polarimetric applications since its variance does not change with the rotation of its Stokes vector. At present we don't know if this all distinct orbits is equivalent to finding all distinct triangles on the state has generalizations for higher photon numbers. The state's Majorana points are defined by the angles  $\theta_1 = 0$ ,  $\theta_2 = \theta_3 \approx 107.5^\circ$ ,  $\phi_2 = 0$ , and  $\phi_3 \approx 115.47^\circ$ . In contrast, a maximally unpolarized, pure state [27] would have had a vanishing Stokes vector *and* an isotropic variance. The orbit of such state is thus also point-like. However, states unpolarized to second order can only be found for  $N = 4$  and  $N \geq 6$  [27].

In conclusion, we have illustrated the permissible Stokes operator variances for all pure states for the  $N = 2$  and  $N = 3$  manifold. The obtained figures are surprisingly involved. Since these operators obey the  $SU(2)$  algebra, all such operators such as angular momentum operators will obey the same, or proportionally scaled, uncertainty volumes. The method is extendible to higher excitation manifolds, but gets progressively difficult. As an example, for the  $N = 4$  excitation manifold, one can define the orbit generating state in the same way as for the  $N = 2$  and  $N = 3$  cases. The orbit generating state will then be a function of 5 parameters and all distinct orbits will correspond to distinct Majorana point quadrilaterals on the Poincaré sphere. The difficulty however lies in defining angular limits that result in distinct orbits. An alternative approach is to generate a point cloud sampled sufficiently densely over all orbits and all polari-

sation transformations (which adds another three parameters). Such an analytically simplistic strategy comes at the expense of significantly increased computation time.

We have highlighted a simple method to check whether states lie on the same  $SU(2)$  orbits and are connected via linear polarisation transformations in terms of the equivalence of their Majorana representations. This provides a first check for identifying realisable quantum experiments [28] excluding post-selection. In this context, consequently, the sum uncertainty relation equation (6) provides useful experimental information; given different values for the uncertainty sum for the initial and required states, one can be sure that (excluding all non-unitary processes such as post-selection etc) there can no be experimental realisation that creates the required

state from the initial.

Lastly, pertaining to mixed states we find that although their uncertainty is also bounded by the limits in (6), they do not always lie inside the shown uncertainty volumes.

## ACKNOWLEDGMENTS

G.B. acknowledges fruitful discussions with Profs. L. L. Sánchez-Soto, and A. B. Klimov. This work was supported by the Swedish Research Council (VR) through grant 621-2014-5410 and through its support of the Linnæus Excellence Center ADOPT.

- 
- [1] D. M. Klyshko, JETP **84**, 1065 (1997).
  - [2] P. Usachev, J. Söderholm, G. Björk, and A. Trifonov, Opt. Commun. **193**, 173 (2001).
  - [3] T. Tsegaye, J. Söderholm, M. Atatüre, A. Trifonov, G. Björk, A. V. Sergienko, B. E. A. Saleh, and M. C. Teich, Phys. Rev. Lett. **85**, 5013 (2000).
  - [4] B. Yurke, S. L. McCall, and J. R. Klauder, Phys. Rev. A **33**, 4033 (1986).
  - [5] D. J. Wineland, J. J. Bollinger, W. M. Itano, and D. J. Heinzen, Phys. Rev. A **50**, 67 (1994).
  - [6] A. Rivas and A. Luis, Phys. Rev. A **77**, 022105 (2008).
  - [7] H. P. Robertson, Phys. Rev. **34**, 163 (1929).
  - [8] E. Schrödinger, Ber. Kgl. Akad. Wiss. Berlin **24**, 296 (1930).
  - [9] D. Trifonov, J. Math. Phys. **35**, 5 (1994).
  - [10] R. R. Puri, Phys. Rev. A **49**, 3 (1994).
  - [11] A. H. El Kinani and M. Daoud, J. Math. Phys. **43**, 714 (2002).
  - [12] L. Maccone and A. K. Pati, Phys. Rev. Lett. **113**, 260401 (2014).
  - [13] B. Chen and S.-M. Fei, Sci. Rep. **5**, 14238 (2015).
  - [14] A. K. Pati and P. K. Sahu, Phys. Lett. A **367**, 177 (2007).
  - [15] A. Wünsche, J. Mod. Opt. **53**, 931 (2006).
  - [16] I. Białynicki-Birula and J. Mycielski, Comm. Math. Phys. **44**, 129 (1975).
  - [17] D. Deutsch, Phys. Rev. Lett. **50**, 631 (1983).
  - [18] H. Maassen and J. M. B. Uffink, Phys. Rev. Lett. **60**, 1103 (1988).
  - [19] G. G. Stokes, Trans. Cambridge Philos. Soc. **9**, 339 (1952), Sec. 19. Reprinted in *Polarized Light*, W. Swindell, ed. (Dowden, Hutchinson and Ross, 1975), pp. 124141.
  - [20] E. Collett, Am. J. Phys. **38**, 563-574 (1970).
  - [21] W. Feller, *An introduction to probability theory and its applications*, vol. 1, 3rd Edition, John Wiley & Sons (1970). ISBN 978-0-471-25709-7.
  - [22] G. Björk, J. Söderholm, Y.-S. Kim, Y.-S. Ra, H.-T. Lim, C. Kothe, Y.-H. Kim, L. L. Sánchez-Soto, and A. B. Klimov, Phys. Rev. A **85**, 053835 (2012).
  - [23] E. Majorana, Nuovo Cimento **9**, 43 (1932).
  - [24] J. Zimba, Elect. J. Theor. Phys. **3**, 143 (2006).
  - [25] H. Hofmann, Phys. Rev. A, **70**, 023812 (2004).
  - [26] S. Shabbir, M. Swillo, and G. Björk, Phys. Rev. A **87**, 053821 (2013).
  - [27] G. Björk, M. Grassl, P. de la Hoz, G. Leuchs and L. L. Sánchez-Soto, Phys. Scr. **90**, 108008 (2015).
  - [28] M. Krenn, M. Malik, R. Fickler, R. Lapkiewicz, A. Zeilinger, arXiv:1509.02749 (2015) [quant-ph].